

# Observations on Electromagnetic Bias in Radar Altimeter Sea Surface Measurements

EDWARD J. WALSH<sup>1</sup> AND FREDERICK C. JACKSON

*NASA Goddard Space Flight Center, Greenbelt, Maryland*

ENZO A. ULIANA

*Naval Research Laboratory, Washington, D. C.*

ROBERT N. SWIFT

*EG&G Washington Analytical Services Center, Inc., Pocomoke City, Maryland*

Because the relative radar cross section of the sea surface increases below mean sea level and decreases above it, the range measurements of satellite radar altimeters are biased toward the wave troughs. Published and unpublished direct measurements of this electromagnetic (EM) bias are examined as well as the predictions of theoretical developments. The EM bias is predominantly a function of the radar frequency used, averaging 1.2% of the wave height of  $K_u$  band and 3.3% of the wave height at X band. The airborne measurements present a consistent picture of the variation of the relative radar cross section as a function of deviation from mean sea level. A technique to measure EM bias at the  $K_u$  and C band operating frequencies of the TOPEX satellite altimeter is described.

## 1. INTRODUCTION

In 1970, B. S. Yaplee and his coworkers at the Naval Research Laboratory (NRL) conducted a milestone experiment using a nanosecond pulse width radar system operating at 10 GHz [Yaplee *et al.*, 1971]. They demonstrated that the sea surface radar cross section per unit area varies with displacement from the mean water level, being smaller toward the crests and larger toward the troughs. They pointed out that the varying reflectivity shifted the electromagnetic centroid away from mean sea level (MSL) toward the troughs and showed that this electromagnetic (EM) bias would affect the range measurements of any radar altimeter that did not illuminate an area small enough to resolve individual ocean waves [Shapiro *et al.*, 1972].

The main goal of satellite radar altimeters is to determine the range to MSL. Because the minimum area they illuminate is several kilometers in diameter, their range measurements are subject to EM bias. The ability to model and predict the magnitude of the EM bias is critical to the Ocean Topography Experiment (TOPEX). The TOPEX altimeter will be part of a U.S. and French joint mission called TOPEX/POSEIDON in which a U.S. satellite will carry both U.S. and French instrumentation. The satellite is scheduled for launch in 1992 by a European Ariane launch vehicle provided by France. The TOPEX altimeter mission requires determination of MSL to an accuracy of a few centimeters. Because there have been no open-ocean measurements of the EM bias at either of the C band or  $K_u$  band operating

frequencies of the TOPEX altimeter, this bias is one of the major uncertainties in the TOPEX error budget.

EM bias observations have been made at 10 GHz [Yaplee *et al.*, 1971; Shapiro *et al.*, 1972; Choy and Uliana, 1980; Choy *et al.*, 1984], at 36 GHz [Kenney and Walsh, 1978; Walsh *et al.*, 1984] and at UV [Hoge *et al.*, 1984] and visible wavelengths. There have been theoretical studies [Miller and Hayne, 1972; Jackson, 1979; Lipa and Barrick, 1981; Huang *et al.*, 1984; Barrick and Lipa, 1985; Srokosz, 1986, 1987; Dudis, 1986; Lagerloef, 1987; Rodriguez, 1988; F. C. Jackson, A two-scale model of the altimeter EM bias, submitted to *Journal of Geophysical Research*, 1989]. Inferences on the magnitude of EM bias have been drawn from laboratory measurements of the joint probability density function (pdf) of the slope and elevation of the water surface [Huang *et al.*, 1984] and from on-orbit measurements from radar altimeters such as GEOS-3 and Seasat [Lipa and Barrick, 1981; Born *et al.*, 1982; Douglas and Agreen, 1983].

The major concerns with respect to EM bias are to determine, for each radar frequency of interest, (1) the mean value, (2) the standard deviation from that mean value, (3) the possibility of parameterizing the variation of the bias (especially in terms of quantities measurable by a satellite altimeter or other space sensor), and (4) the residual uncertainty in the bias after parameterization.

The main points of this paper are that (1) it is not possible to eliminate EM bias in satellite altimeter measurements solely on a basis of return waveform processing, (2) EM bias shows a strong dependence on the wavelength of the incident radiation, (3) all theoretical analyses of EM bias to date have obvious limitations since they fail to predict the frequency dependence, (4) theoretical developments based on the Gram-Charlier series expansion fail to predict anything more sophisticated than a linear variation of relative radar cross section with deviation from mean sea level, (5) the only

<sup>1</sup>On assignment at NOAA Wave Propagation Laboratory, Boulder, Colorado.

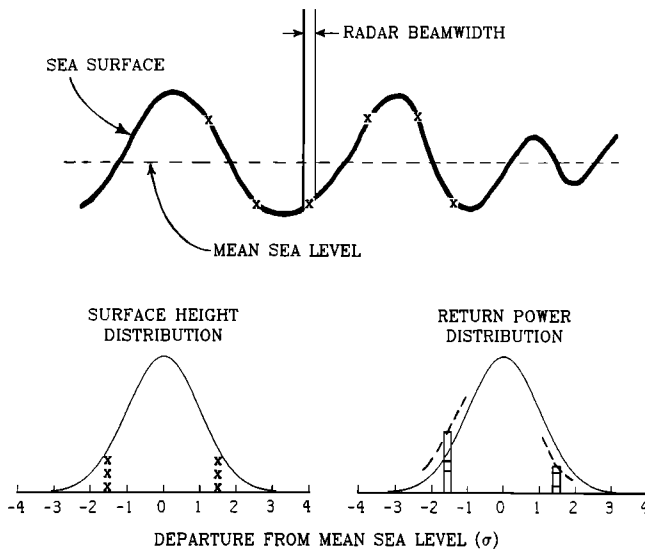


Fig. 1. Schematic representation of EM bias measurement.

tower measurements to date exhibit peculiarities which raise questions as to whether such near-surface measurements can be used to predict the EM bias effects in satellite altimeter measurements, and (6) measurements at  $C$  and  $K_u$  band are needed to resolve the EM bias problem for the TOPEX altimeter.

## 2. EM BIAS EFFECT ON RADAR RETURN WAVEFORMS

To determine the EM bias at a given radar frequency, it is necessary to make simultaneous high-spatial-resolution measurements of the elevation and backscattered power. The illuminated spot must be small compared with the dominant ocean wavelength and the range resolution must be high compared to the significant wave height (SWH), taken to be equal to 4 times the sea surface height standard deviation ( $\sigma$ ). From the measurements, two distributions are developed whose abscissas are elevation.

Figure 1 illustrates the measurement situation schematically. Suppose that an airborne radar with a narrow beam profiles the waves below it. For each range measurement made by the radar the "surface height" distribution increases by one unit at the observed elevation. This is indicated by the six X marks, three corresponding to observations near the crests and three near the troughs. The "return power" distribution also increases at the observed elevation bin, but by the amount of the measured backscattered power. Statistically, the three observations of power near the troughs would have a higher average than the three observations near the crests. This is because  $\sigma_{rel}^o$ , the sea surface relative radar cross section per unit area, is higher near the troughs than it is near the crests.

Figure 2 demonstrates how the average radar return power would be affected for different linear variations of  $\sigma_{rel}^o$  with distance from MSL. This assumption, first employed by Miller and Hayne [1972], simplifies the computations and gives insight into two important points. First, the EM bias is approximately proportional to the slope of the  $\sigma_{rel}^o$  curve. Second, without prior knowledge it is not possible to determine and eliminate the EM bias by using waveform processing on the altimeter return. The only way to eliminate EM

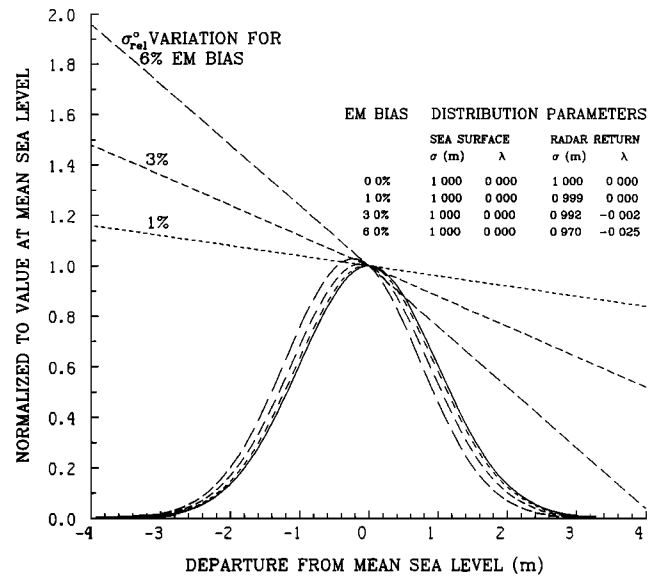


Fig. 2. Return power distributions (dashed curves) corresponding to the same sea surface height distribution (solid curve) assuming that  $\sigma_{rel}^o$  varies linearly with deviation from MSL for various values of EM bias.

bias from a satellite altimeter range measurement is to have already determined it independently through airborne or tower measurements or by theory.

The return waveform of a satellite radar altimeter resembles a cumulative normal distribution whose plateau droops [Brown, 1977; Hayne, 1980]. Figure 2 shows four approximately normal distributions that can be considered to be the result of taking a satellite altimeter return waveform and deconvolving the effect of the antenna pattern. If the antenna pattern were broad enough for there to be no plateau droop in the return waveform, the procedure would be equivalent to differentiating the leading edge of the return. The result is the variation of return (backscattered) power as a function of distance from MSL.

The four curves in Figure 2 representing radar return power distributions were arrived at from a single sea surface height distribution. The solid curve represents both the backscattered power distribution for the case of no EM bias and the sea surface height distribution. It is a Gaussian curve with zero skewness and 1 m standard deviation corresponding to a 4-m SWH. When  $\sigma_{rel}^o$  does not vary with distance from MSL, the radar return power distribution is identical in shape and position to the sea surface height distribution and the radar will determine the position of MSL.

The three dashed curves represent the backscattered power when the  $\sigma_{rel}^o$  variation corresponds to the three dashed straight lines. The backscattered power curves were obtained by multiplying the surface height distribution (solid curve) by the value of  $\sigma_{rel}^o$  from the corresponding dashed straight line. As the slope of the straight-line  $\sigma_{rel}^o$  variation increases, it induces EM biases (shift of the centroid of the radar return away from MSL toward the troughs of the waves) of 1%, 3%, and 6% of the SWH. Along with the shift in the centroid (4, 12, and 24 cm), it is also apparent in Figure 2 that the amplitude of the radar return increases slightly as the EM bias increases.

There are also more subtle changes in the radar return, which are indicated in the table in Figure 2. The standard

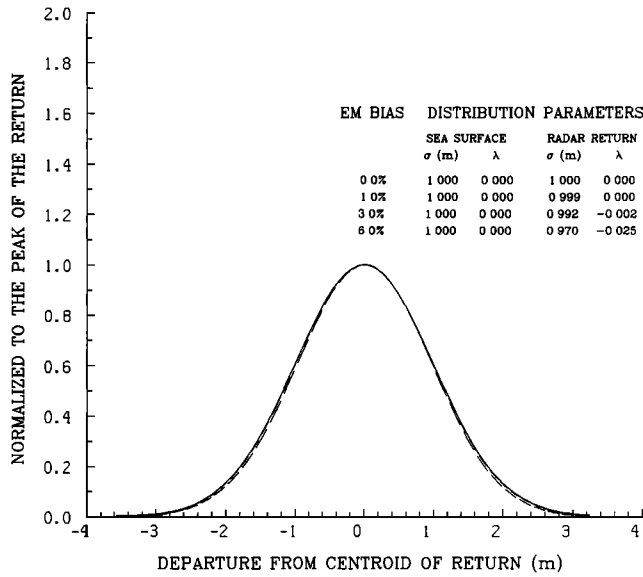


Fig. 3. The four return power distributions of Figure 2, after they have been normalized to their peak values and plotted with respect to their centroids.

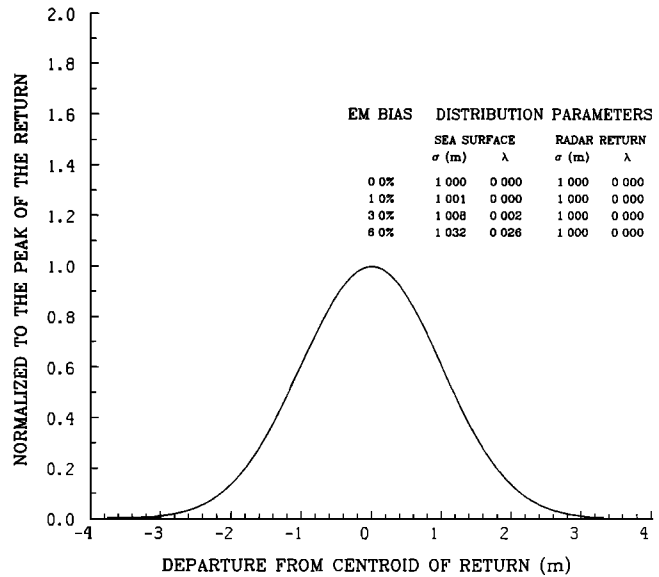


Fig. 5. The four return power distributions of Figure 4, after they have been normalized to their peak values and plotted with respect to their centroids.

deviation of the radar return decreases slightly as the EM bias increases, and the skewness of the radar return becomes slightly negative. Figure 3 shows how the radar would present the four returns, normalized to their peak values and their ranges adjusted to their respective centroids. The slight differences in the parameters of the four distributions are more apparent in this representation. But one could not hope to use these slight changes in shape to determine the EM bias. This is demonstrated by Figures 4 and 5.

Figure 4 appears to be very similar to Figure 2. But in Figure 4 the parameters of the sea surface height distribution were changed slightly for each different  $\sigma_{rel}^0$  variation. The result was that the centroids of the three dashed distributions were still shifted approximately 4, 12, and 24 cm away from

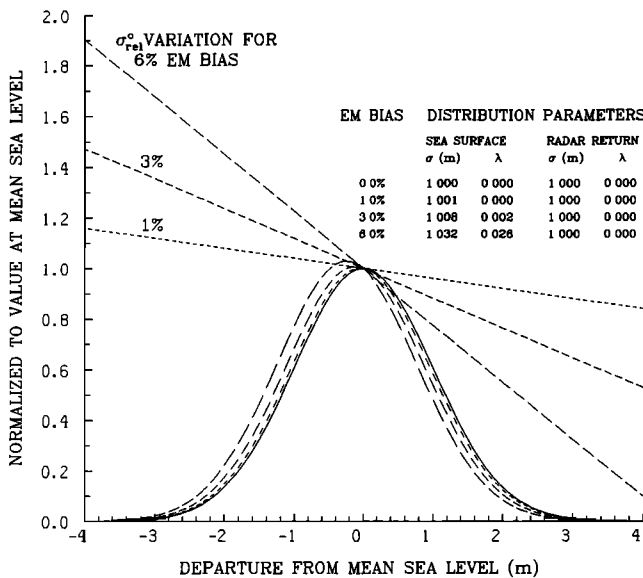


Fig. 4. Return power distributions corresponding to slightly different sea surface height distributions so that the return power distributions have the same standard deviation and skewness.

MSL towards the troughs, but the shape parameters of the resulting backscattered power distributions were identical (zero skewness and 1-m standard deviation). This effect is more apparent in Figure 5, which is similar to Figure 3 except the four waveforms overlie almost exactly. The radar would think it was seeing the same return although the bias in the range measurement could be anywhere from 0 to 24 cm. The kurtosis of the backscattered power distributions also varies slightly as the EM bias changes, but it was not included in the parameterization. Had it been, the curves in Figure 5 would have agreed even better. Rodriguez [1988] has also pointed out the practical impossibility of trying to determine the EM bias directly from a satellite altimeter return waveform.

Figure 5 indicates that one has to know a priori the magnitude of the EM bias and apply a correction for it accordingly. The skewness and kurtosis of the return waveform may offer some clues to the EM bias correction, as may the altimeter measurement of the wind speed in comparison with the wave height (is it a developing sea or is it swell?). But the magnitude and parameterization of EM bias must be established by an independent airborne or tower measurement program.

The surface contour radar (SCR) operates at 36 GHz [Kenney et al., 1979]. Walsh et al. [1984] observed that EM bias data acquired on the same day tended to cluster and suggested that EM bias might be parameterized to reduce the effect of its variability. Figures 6, 7, and 8 show scatter plots of EM bias as functions of SWH, surface height skewness, and wave steepness for 36-GHz and 10-GHz observations. The data points are a composite of the information of Walsh et al. [1984] and Choy et al. [1984] with additional observations under steep wave conditions added to the earlier 36-GHz data set. The previously unpublished SCR observations were both made offshore of Wallops Flight Facility (37.8°N, 75.6°W) in April 1978. On April 14, there was a NW wind at 10 m/s developing fetch-limited waves. When the waves had grown to a SWH of 1.56 m (0.077 surface height

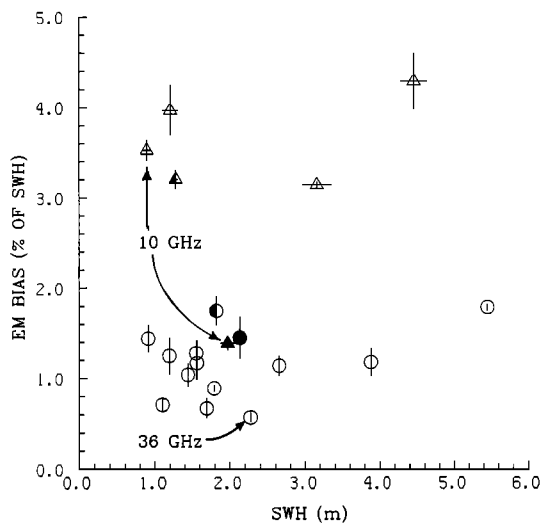


Fig. 6. EM bias versus wave height for airborne observations. Circles indicate 36-GHz observations [Walsh *et al.*, 1984]; triangles indicate 10-GHz observations [Choy *et al.*, 1984]. The solid symbols show observations from the same flight; the half solid symbols show observations made from different aircraft on the same day.

skewness, 2.92 kurtosis, 44-m wavelength) the EM bias was measured to be 1.17% of SWH (hereinafter EM bias will be referred to simply as a percentage with the understanding that it is referenced to the SWH). On April 27 a northeaster was blowing, with the wind speed at the time of flight being 16 m/s although it was 21 m/s only 8 hours before the flight. The SWH was 5.45 m (0.140 surface height skewness, 2.93 kurtosis, 157-m wavelength) and the EM bias was measured to be 1.79%.

The symbols in Figure 6 indicate the average of the observations on a given day, and the calculated 1- $\sigma$  error bars on each average value are indicated by the horizontal and vertical lines. No wave height error bars are shown for

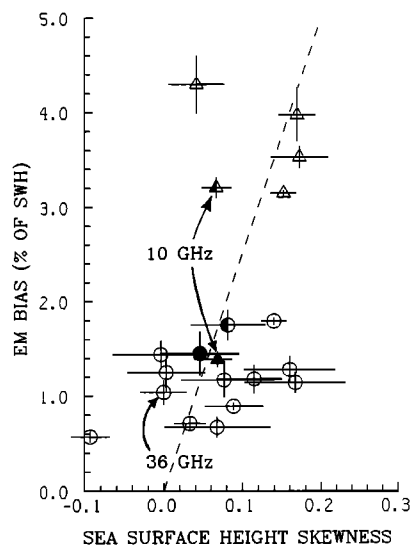


Fig. 7. EM bias versus surface height skewness for airborne observations. Circles indicate 36-GHz observations [Walsh *et al.*, 1984]; triangles indicate 10-GHz observations [Choy *et al.*, 1984]. The dashed line indicates the theoretical relation between the EM bias and the skewness of a pure sea having a Phillips cutoff  $k^{-3}$  spectrum [Jackson, 1979].

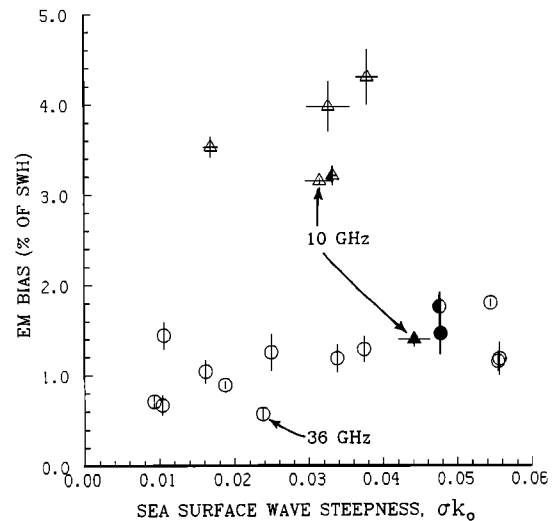


Fig. 8. EM bias versus wave steepness for airborne observations. Circles indicate 36-GHz observations [Walsh *et al.*, 1984]; triangles indicate 10-GHz observations [Choy *et al.*, 1984].

the 36-GHz observations, since they were generally smaller than the symbol size. There was one day when the NRL radar was the NASA aircraft along with the SCR; the corresponding symbols are solid. In another instance the two instruments were on different aircraft but flew off Wallops Flight Facility on the same day. The left sides of those symbols are shaded.

Neither frequency shows any significant trend of EM bias with wave height. That should not be surprising since a given wave height could correspond to a sea state that was either steep wind-driven waves or a gentle swell propagating in a region of low wind.

Figure 7 shows a scatter plot of EM bias versus the skewness of the surface height distribution for 36 GHz and 10 GHz. There is a significant amount of scatter in the data and no clear trend.

Figure 8 shows a scatter plot of EM bias versus  $\sigma k_0$ , a measure of the steepness of the waves at the spectral peak. With  $k_0$  being the wave number at the peak of the spectrum,  $\sigma k_0$  would be the root-mean-square sea surface slope for a narrow band swell system. Wave steepness is generally assumed to be a measure of the nonlinear characteristics of a wave system, with developing seas being steeper than fully developed sea states, which in turn are steeper than swell. The wave steepness parameter used here is a factor of  $2\pi$  larger than the "significant slope" term defined by Huang and Long [1980] and shown by Huang *et al.* [1981, 1983, 1984, 1986] to be highly correlated with many statistical properties of the wave field. The SCR data exhibit a slight increase of EM bias with wave steepness.

The trend in the SCR observations in Figure 8 is small compared with the difference in the mean values of the 10-GHz and 36-GHz data sets. At 36 GHz the average EM bias is 1.2%, whereas at 10 GHz it is 3.3%.

The EM bias measurements at the two frequencies are almost disjoint. It is unfortunate that the one observation out of six at 10 GHz which was comparable to the 36 GHz measurements occurred when both instruments were on the same aircraft. But this must be viewed as coincidence. The  $t$  test of significance for the 20 EM bias values of the 10-GHz

and 36-GHz observations is 1.97, indicating that there is only about a 5% chance that they could have been samples from the same distribution.

But the case for frequency dependence in EM bias is made even stronger when it is noted that the range of wave heights covered by the 36-GHz observations exceeds that of the 10-GHz measurements, as do the range of wave steepness values and the range of wind speeds. That means that the range of EM bias values at 36 GHz should have exceeded those at 10 GHz if there were no frequency dependence. Even so, none of the 36-GHz observations exceeds 1.8%. The standard deviation of the 36-GHz EM bias values is 0.36, so that five of the six observations at 10 GHz are more than 5 standard deviations from the mean of the 36 GHz observations. The conclusion that must be drawn is that the most significant characteristic of EM bias is that it increases as the radar frequency is decreased from 36 GHz to 10 GHz.

### 3. THEORETICAL RADAR CROSS SECTION VARIATION

Present theory of EM bias is based on the geometrical optics approximation to backscatter [Barrick, 1972], according to which the average radar return power  $\eta(z)$  is proportional to the joint probability density function of wave height and slope, where the slope satisfies the specular condition for backscatter, namely, slope = 0. There is an inherent problem in the geometric optics approach in that it considers all of the horizontal facets in the wave field to be perfect reflectors and therefore cannot account for the pronounced radar frequency dependence seen in the preceding section. This limitation brings into question the quantitative predictive value of these developments and indicates the need for a more sophisticated approach to this scattering problem. We will also see that the Gram-Charlier approach used in many of the theoretical developments produces nothing more subtle qualitatively than the linear variation of  $\sigma_{rel}^o$  assumed in Figures 2 and 4.

The theoretical developments of Jackson [1979], Barrick and Lipa [1985], and Srokosz [1986] are all based on Longuet-Higgins' [1963] statistical theory for free gravity waves, all truncate the Gram-Charlier (G-C) series expression for the joint pdf at the third degree, and all yield an identical form for the radar return power, namely,

$$\eta(z) = \frac{\sigma^o}{(2\pi)^{1/2}\sigma} \exp(-Z^2/2) * h(Z) \quad (1)$$

where  $Z = z/\sigma$ ,  $z$  being the vertical displacement relative to MSL, and

$$h(Z) = 1 + \frac{\lambda_1}{6} * (Z^3 - 3Z) - \lambda_2 Z/2 \quad (2)$$

where  $\lambda_1$  and  $\lambda_2$  are the height and the "height and slope squared" skewness coefficients, respectively. The conventional surface radar cross section is given by

$$\sigma^o = \int_{-\infty}^{\infty} \eta(z) dz \quad (3)$$

Consistent with the truncated form of (1), the height pdf is

$$f(z) = \frac{1}{(2\pi)^{1/2}\sigma} \exp(-Z^2/2) * g(Z) \quad (4)$$

where

$$g(Z) = 1 + \frac{\lambda_1}{6} * (Z^3 - 3Z) \quad (5)$$

Since these expressions are referenced to MSL, the EM bias in absolute units is just the centroid of the return power distribution.

EM bias (absolute units)

$$= \frac{1}{\sigma^o} \int_{-\infty}^{\infty} \eta(z)z dz = -\lambda_2\sigma/2 \quad (6)$$

and the value normalized by SWH and referenced toward the troughs is

$$\text{EM bias (normalized by SWH)} = \lambda_2/8 \quad (7)$$

The normalized conditional or relative cross section versus deviation from MSL is given by

$$\sigma_{rel}^o(z) = \frac{\eta(z)}{\sigma^o * f(z)} = \frac{h(Z)}{g(Z)} \quad (8)$$

$$\sigma_{rel}^o(z) = 1 - \lambda_2 Z/2 + \dots \quad (9)$$

Equation (9) indicates that to a first approximation the relative cross section varies linearly with deviation from MSL and, combined with (7), shows that the fractional bias is determined by the slope of  $\sigma_{rel}^o$  at  $z = 0$  [Jackson, 1979].

For the case of a one-dimensional unidirectional Phillips wind-sea spectrum, Jackson [1979] found  $\lambda_2 = 2\lambda_1$ ; for a pure swell, Jackson's [1979] theory gives  $\lambda_2 = \lambda_1$  [Dudis, 1986]. For the Phillips spectrum case,  $\lambda_1 = 0.20$ , in which case the bias predicted by Jackson is 5% of SWH. Barrick and Lipa [1985], on the other hand, found a bias of about 3% of SWH for a two-dimensional Joint North Sea Wave Project (JONSWAP) spectrum; however, they did not report their results for the relationship between  $\lambda_1$  and  $\lambda_2$ . Generally, according to these theories, one cannot predict the relationship between  $\lambda_1$  and  $\lambda_2$  without a priori knowledge of the directional wave spectrum. If one could, then in principle one could predict the bias from the measured skewness of the return waveform [Jackson, 1979; Rodriguez, 1988].

Figure 9 shows plots of  $g(Z)$  and  $f(Z)$ . It is seen in (8) that the expression for  $\sigma_{rel}^o(z)$  contains  $g(Z)$  in the denominator, and therein lies a problem. Figure 9 shows that  $f(Z)$  is not actually a pdf because the factor  $g(Z)$  becomes and remains negative at some point below MSL for nonzero skewness. The result is that  $\sigma_{rel}^o(z)$  will contain a singularity where  $f(Z)$  goes through zero.

Figure 10 plots  $\sigma_{rel}^o(z)$  calculated from (8) for a fixed nominal value of EM bias of 3% ( $\lambda_2 = 0.24$ ) for several values of  $\lambda_1$ . For the parameter values given, all the curves are approximately linear between  $z = -2\sigma$  and  $z = 2\sigma$ . Above  $3\sigma$  the relative cross section increases slightly; below  $-3\sigma$  it rises rapidly as the singularity is approached. To the left of the singularity the curves are negative until  $h(Z)$  become positive again because the backscattered power and the height distribution are both negative, neither of which is physically realizable. Clearly, nothing to the left of the singularity means anything. The question arises whether the curves turning up outside the linear region ( $-2\sigma$  to  $2\sigma$ ) are physically realistic or also merely an artifact of the trunca-

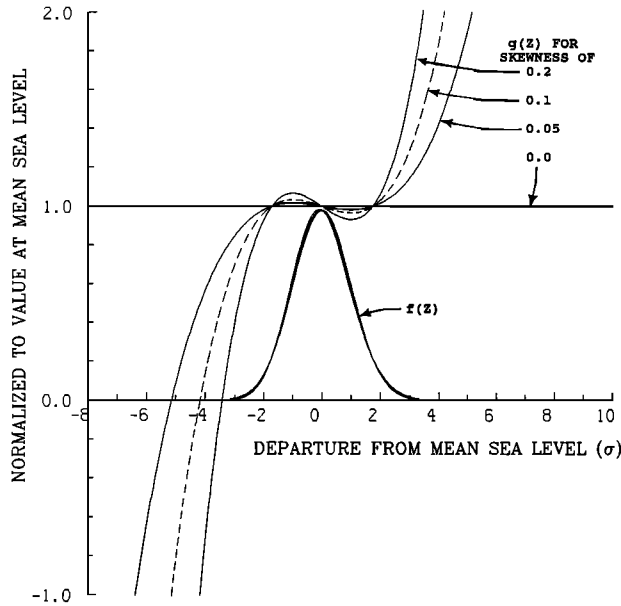


Fig. 9. Plots of  $g(z)$  and  $f(z)$ . The  $f(z)$  plots are multiplied by 0.98 to avoid confusion between curves at MSL.

tion of the G-C series. We postpone discussion of this matter until section 4. Figure 11 shows that the G-C development predicts a virtually linear variation of  $\sigma_{rel}^o$  between  $-2\sigma$  and  $2\sigma$  even for a 6% EM bias.

Huang *et al.* [1983, 1984] developed series expansion solutions in terms of  $ak$  (where  $a$  is wave amplitude and  $k$  is wave number) for the height and joint height-slope pdf's of a narrowband Stokes wave. To be valid, the combination of displacement from MSL and  $ak$  must be small. Despite the questions raised by Tayfun [1986] on the validity of their approximate development, N. E. Huang (private communication, 1989) still believes that their expression for  $\sigma_{rel}^o(z)$  has validity. It is only a function of wave steepness and never

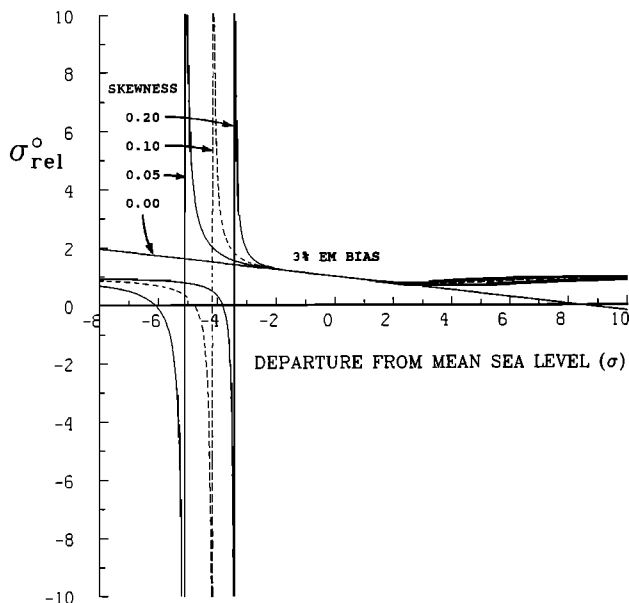


Fig. 10. Plots of  $\sigma_{rel}^o$  calculated from the truncated Gram-Charlier series for a 3% EM bias and several values of sea surface height skewness.

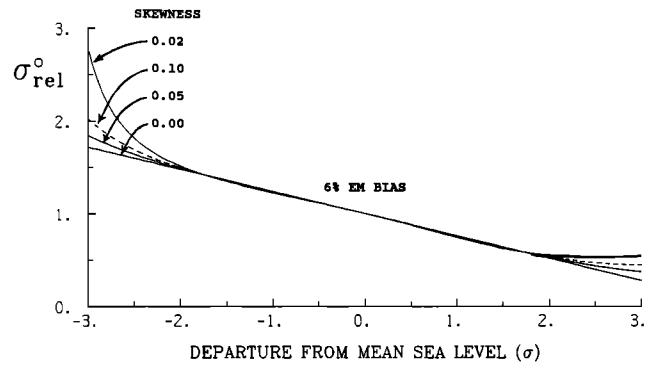


Fig. 11. Plots of  $\sigma_{rel}^o$  calculated from the truncated Gram-Charlier series for a 6% EM bias and several values of sea surface height skewness.

goes negative. However, it can still attain very large values below MSL, as is shown in Figure 12. The three values of wave steepness ( $\sigma k$ ) were selected to match the slope at MSL of the linear  $\sigma_{rel}^o(z)$  variations shown in Figure 4 for EM bias values of 1%, 3%, and 6%. Figure 13 is a blow-up of Figure 12 near MSL. The curve whose slope at MSL corresponds to a 6% EM bias for a linear  $\sigma_{rel}^o$  variation shows a significant amount of nonlinearity.

#### 4. MEASURED RADAR CROSS SECTION VARIATION

The available nadir observations of EM bias are divided between a limited number of tower data at  $X$  band and aircraft data at  $X$  and  $K_a$  band and optical frequencies. Figure 14 shows the variation of  $\sigma_{rel}^o$  for two different sea states at 36 GHz. The curves, obtained by dividing the return power distribution by the surface height distribution, are very similar for the two wave heights and indicate that  $\sigma_{rel}^o$  is higher for the portion of the sea surface below MSL than for the portion above. The curves are very similar out to 2.5 standard deviations, after which there are relatively few data points and the statistical fluctuations become large. The data indicate a very smooth variation in  $\sigma_{rel}^o$ .

Figure 15 shows the normalized radar cross section curves measured by Yapple *et al.* [1971] in their 10-GHz tower experiment. The curves show an impressive similarity even though one was for a calm wind and 1-m wave height and the other was for a 10.5-m/s wind and 1.6-m wave height. This again emphasizes that EM bias is mainly a function of radar

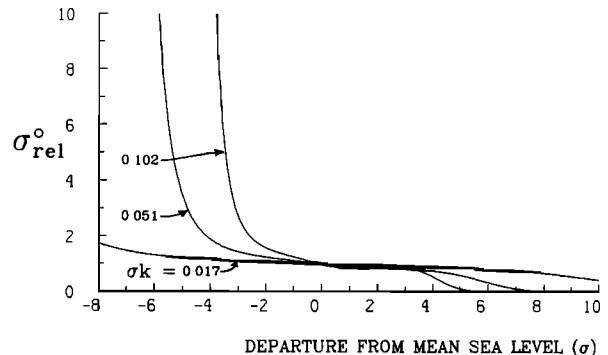


Fig. 12. Plots of  $\sigma_{rel}^o$  calculated from a narrowband Stokes wave series expansion [Huang *et al.*, 1983, 1984] for several values of wave steepness.

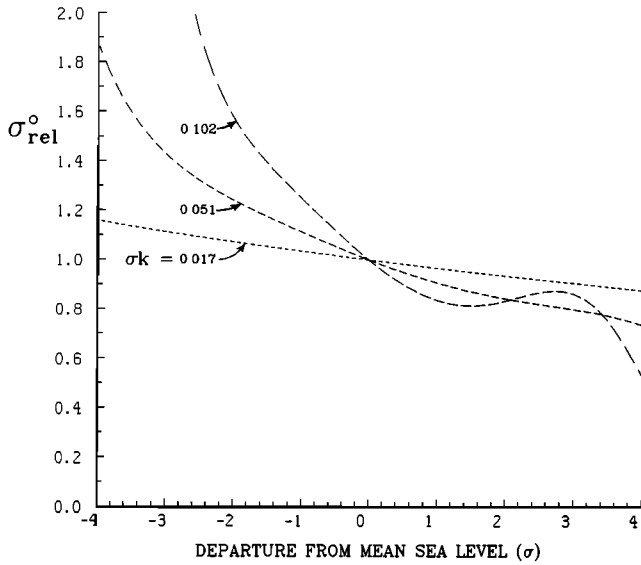


Fig. 13. An expansion of Figure 12 around MSL.

wavelength. However, the curves have some disturbing characteristics.

In addition to the basic trend of increasing cross section with depth into the waves, the slope of the curves appears to change abruptly at MSL, and there are local maxima in the vicinity of  $1.5\sigma$  and  $-1.5\sigma$ . Beyond 2 standard deviations from MSL the cross section drops abruptly, giving an overall negative curvature or convex shape to the cross section between  $-3\sigma$  and  $3\sigma$ .

The tower data were obtained at a height of 20 m above mean water level, and it is possible that near-field effects are influencing the data. The entire spot,  $\sim 0.7$  m in diameter, is within the first Fresnel zone, and it is therefore possible that coherent returns from flatter portions of the sea surface near the crests and troughs are enhancing the tower cross section data near  $1.5\sigma$  and  $-1.5\sigma$ . *LeVine* [1982] showed that proximity effects can increase the measured cross section relative to the far-field cross section, but it is not clear how this effect could preferentially enhance crest and trough regions.

Figure 15 should be contrasted with Figure 16, which shows the  $\sigma_{rel}^0$  variations for two airborne data sets collected

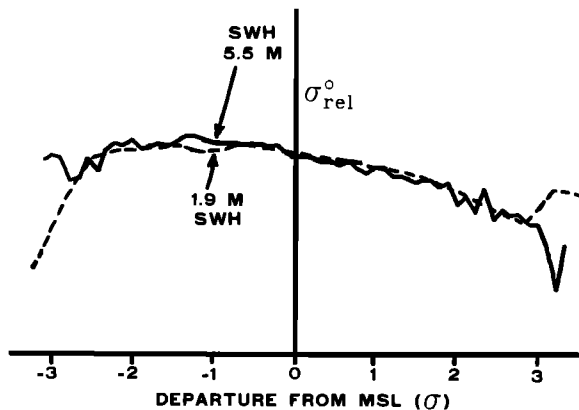


Fig. 14. Average  $\sigma_{rel}^0$  variation for SCR measurements made at a 5.5-m SWH and a 1.9-m SWH [Walsh et al., 1984].

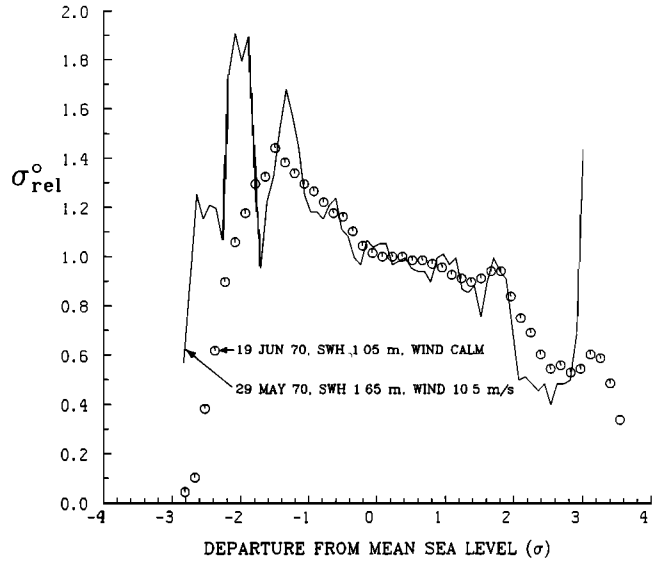


Fig. 15. NRL tower measurements of  $\sigma_{rel}^0$  at 10 GHz [Yaplee et al., 1971].

by NRL at 10 GHz. One corresponds to a measured EM bias of 3% for a 3.1-m SWH, and the other is for a measured EM bias of 4% for a 2.4-m SWH. The shapes of these two  $\sigma_{rel}^0$  variations are very similar, but they are smoothly varying and do not evidence the disturbing features of the tower data shown in Figure 15.

Figure 17 shows four curves that were developed from laser profile data taken on October 8, 1984 in the vicinity of ( $55^\circ\text{S}$ ,  $80^\circ\text{W}$ ), approximately 400 km off the coast of Chile. The airborne oceanographic lidar (AOL) was using a pulsed frequency doubled Nd:YAG laser operating in the blue-green portion of the spectrum (532 nm). The wind was from the west at about 25 m/s at the 800-m altitude where the data were taken, but it would not be reliable to attempt to extrapolate the wind speed at that altitude to a value at the sea surface. The indications are that the sea surface wind was considerably lower. Analysis of NOAA 7 cloud imagery

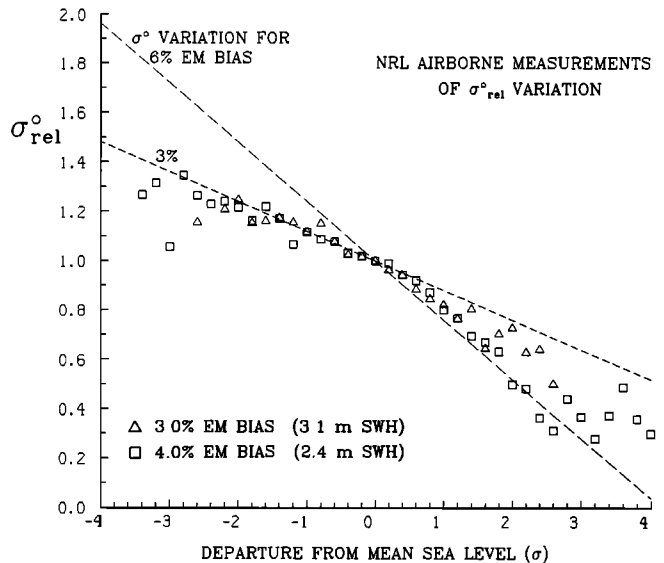


Fig. 16. NRL airborne measurements of  $\sigma_{rel}^0$  at 10 GHz.

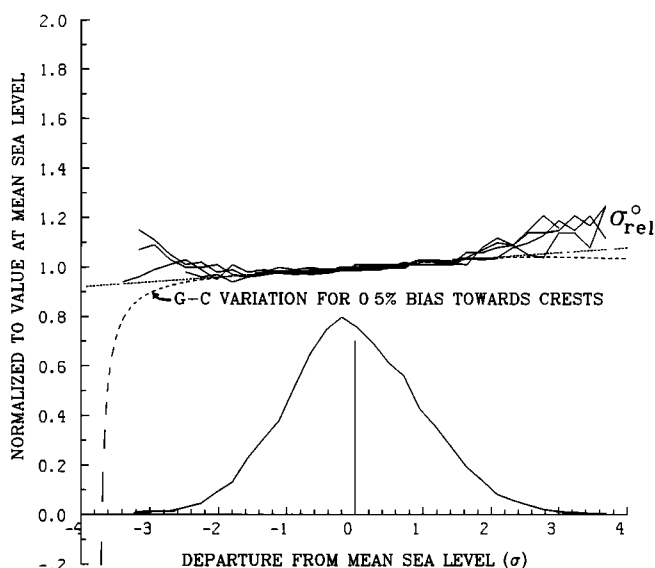


Fig. 17. AOL airborne measurements of  $\sigma_{rel}^o$  in the visible. The surface height distribution for all the points is shown at the bottom with its peak normalized to 0.8.

indicates no significant weather fronts near the data collection area on that day. There was certainly some swell present, and the total wave height measured by the AOL was only 4.2 m, which could have been generated by a wind speed as low as 14 m/s. The Fleet Numerical Oceanography Center (FNOC) global spectral ocean wave model (GSOWM) indicated that at the time of the data collection, the wave height at (55°S, 77.5°W) was 4.4 m and the wind speed was 12.6 m/s from 236°.

The laser pulse repetition frequency (prf) was 100 Hz, and each of the four curves was developed from contiguous, nonoverlapping data sets of approximately 1 min duration. Each of the surface height distributions contained approximately 5800 points. The surface height distribution for all the points in the four data sets is shown at the bottom. As was the case with the other frequencies of observation, these curves show a remarkable consistency. However, in this instance the bias is toward the crests of the waves instead of the troughs, as was the case for the microwave observations.

For comparison, the slope corresponding to a 0.5% bias toward the crests is indicated by a dotted straight line. Also indicated is the predicted G-C variation (equation (8)) for the same bias and the measured 0.14 height skewness. Where the G-C curve deviates from a straight line it deviates in the wrong direction compared with the observations. This was also the situation for all the aircraft microwave observations as well (see Figure 10 and Figures 14 and 16). The data shown in Figure 17 are typical of the AOL observations on that day. But in one 2-min segment the EM bias was zero and  $\sigma_{rel}^o$  was virtually a horizontal straight line with no curvature at all.

From the 800-m altitude of the AOL data acquisition, the illuminated spot was  $\sim 2$  m in diameter. At the 190-m to 564-m altitude range where the 36-GHz aircraft data were obtained, the illuminated spot varied from approximately 4 m to 12 m, increasing with the dominant ocean wavelength. The 10-GHz aircraft data were acquired at 150 m to 230 m altitude, and the illuminated spot varied from 11 m to 17 m in diameter. Considering the dominant ocean wave lengths

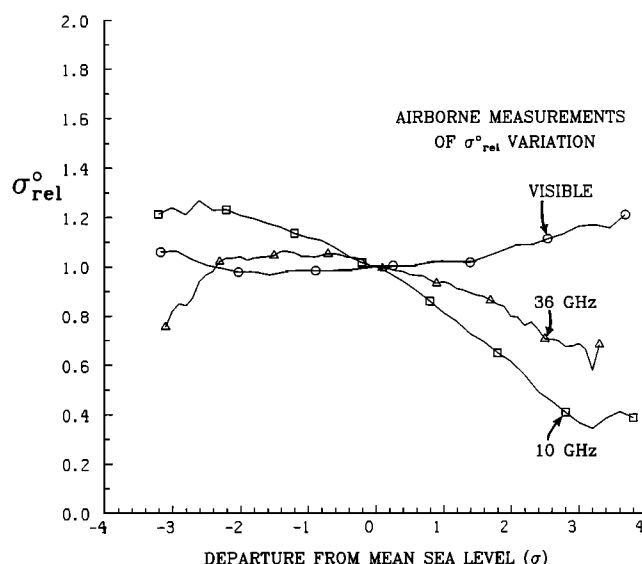


Fig. 18. Average behavior of the airborne measurements of  $\sigma_{rel}^o$  at visible frequency, 36 GHz, and 10 GHz.

involved (44 m to 256 m for the SCR, 60 m to 250 m for the 10 GHz measurements), *Choy et al.* [1984] have shown that none of the airborne  $\sigma_{rel}^o$  observations was corrupted by spatial filtering from the footprint.

The curves in Figure 18 are the averages of the airborne observations shown in Figures 14, 16, and 17. Before being plotted in Figure 18, the data of Figure 16 were smoothed by a three-point moving average to reduce the fluctuations. To first order, one could consider the  $\sigma_{rel}^o$  variation to be perfectly linear, and increasing EM bias would simply result from steepening the slope of the straight line. But these curves seem to indicate that the  $\sigma_{rel}^o$  variation deviates from a straight line in a fashion that is nearly independent of operating frequency and that higher EM bias simply means a higher mean slope for the same shaped curve.

All three curves in Figure 18 have about the same amount of curvature, and they show a steepening slope above MSL. It appears that the observations are consistent enough to be used as a standard to compare the theoretical predictions against. Since the curvature of the G-C development was opposite to the aircraft observations in all cases, it appears that where the G-C development deviates from a straight line outside the interval from  $-2\sigma$  to  $2\sigma$  it is not physically realistic and is simply an artifact of the truncation of the G-C series. The G-C development is essentially just predicting the slope of the straight line within the  $-2\sigma$  to  $2\sigma$  interval and not describing any higher-order characteristic of the variation of the radar cross section. These preliminary data show great promise, but they are inadequate for sorting out the EM bias effects in the TOPEX altimeter measurements.

Figure 19 shows that if the variation of EM bias were linear with operating frequency, then the average value at the TOPEX operating frequencies would be about 3% at 13.6 GHz and 3.6% at 5.3 GHz. But if the variation were inversely proportional to frequency, then the biases would be about 2.7% at  $K_u$  band and almost 7% at  $C$  band. Figure 2 indicates that a 6% EM bias would require the radar signal returned from the wave troughs ( $-2\sigma$ ) to be almost 3 times greater than that from the crests ( $2\sigma$ ). That is quite a disparity and suggests that the biases will be closer to the

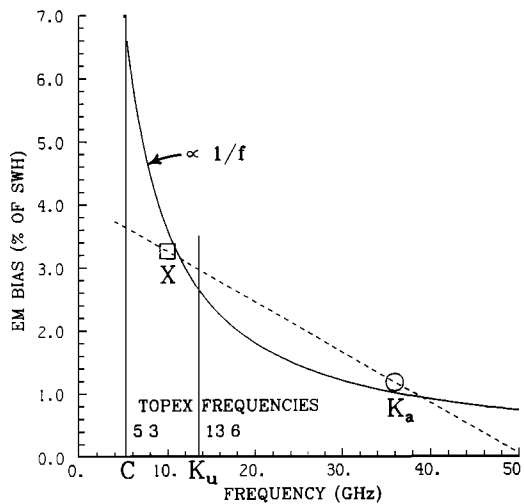


Fig. 19. Average EM bias values for the 10-GHz (square) and 36-GHz (circle) airborne observations, and extrapolation curves assuming linear (dashed curve) and inverse (solid curve) variation with frequency.

linear variation in Figure 19, with  $K_u$  band near 3% and C band near 4%. The magnitude of the  $K_u$  band bias is consistent with inferences obtained from on-orbit satellite altimeter range measurements [Douglas and Agreen, 1983; C. Kobinski, private communication, 1989].

#### 5. MULTIFREQUENCY MEASUREMENT TECHNIQUE

In trying to develop a complete picture of EM bias by comparing measurements from different experiments, there is a corrupting influence of errors in the characterization of the measurement circumstances (such as wind speed and sea state), in addition to errors in the measurement of the bias itself. The optimum situation would be to measure the EM bias simultaneously at several frequencies that illuminated the same spot on the sea surface. Then if there were an error in determining the wind speed it would not affect the relative agreement between the EM bias values for the various frequencies as it would if they were measured in separate localities or even in the same region at different times. This technique would also allow a point-by-point comparison of the variation of the backscattered power from one frequency to another instead of just a comparison of mean results. This capability might be an important aid in investigating the causes of the  $\sigma_{rel}^0$  variation and in improving theoretical models of the EM bias effect.

Although the determination of EM bias requires the simultaneous measurement of elevation and backscattered power, the two measurements do not have to be made with the same instrument. The SCR could measure the ocean surface topography in two dimensions while the backscattered power was being measured simultaneously at other frequencies by instruments which would not even need to measure range. This means that existing instruments such as the 13.9-GHz radar ocean wave spectrometer (ROWS) [Jackson et al., 1985a, b] and the University of Massachusetts C band scatterometer could be combined with the high-quality topographic measurements from the SCR or the AOL to produce simultaneous multifrequency measurements of EM bias.

In addition to the basic measurements of EM bias, such a collection of simultaneous measurements would answer the important question of whether the variability in EM bias is correlated between  $K_u$  and C band. Because of the way the ionospheric range correction is made, if the EM bias variability is correlated between the two frequencies, the overall variability would be reduced to almost half of what it would be if they were uncorrelated.

#### 6. CONCLUSIONS

Airborne observations at 10 GHz, 36 GHz, and optical frequencies indicate that EM bias is predominantly a function of frequency. The bias is toward the troughs for the microwave observations, with a magnitude of about 3.3% of the SWH at 10 GHz and 1.2% at 36 GHz. At optical frequencies the range measurement can be either unbiased or biased toward the crests by about 0.5% of the SWH. The indications are that the TOPEX altimeter will experience an EM bias near 3.0% at its  $K_u$  band operating frequency and near 4% at its C band frequency. The present theoretical developments are inadequate to predict the observed  $\sigma_{rel}^0$  variation with deviation from MSL. Simultaneous measurements of EM bias at the TOPEX operating frequencies are needed to establish optimum corrections for the TOPEX range measurements.

*Acknowledgments.* The authors thank Calvin T. Swift and Robert E. McIntosh of the University of Massachusetts Microwave Remote Sensing Laboratory for discussions concerning the multifrequency measurement technique and Donald E. Barrick for general discussions regarding EM bias. Robert C. Beal is thanked for discussions on the Chile data set. This study was supported by the NASA Oceanic Processes Program.

#### REFERENCES

- Barrick, D. E., Determination of mean surface position and sea state from the radar return of a short-pulse satellite altimeter, *Sea Surface Topography From Space*, edited by J. R. Apel, *Tech. Rep. ERL 228-AOML 7*, vol. 1, pp. 16-1-16-19, Natl. Oceanic and Atmos. Admin., Boulder, Colo., 1972.
- Barrick, D. E., and B. J. Lipa, Analysis and interpretation of altimeter sea echo, *Adv. Geophys.*, **27**, 60-69, 1985.
- Born, G. H., M. A. Richards, and G. W. Rosborough, An empirical determination of the effects of sea state bias on Seasat altimetry, *J. Geophys. Res.*, **87**, 3221-3226, 1982.
- Brown, G. S., The average impulse response of a rough surface and its applications, *IEEE Trans. Antennas Propag.*, **AP-25**, 67-74, 1977.
- Choy, L. W., and E. A. Uliana, Backscattering of narrow radar and laser pulses from a non-Gaussian sea, paper presented at Terrain and Sea Scatter Workshop, George Wash. Univ., Washington, D. C., March 1980.
- Choy, L. W., D. L. Hammond, and E. A. Uliana, Electromagnetic bias of 10-GHz radar altimeter measurements of MSL, *Mar. Geod.*, **8**, 297-312, 1984.
- Douglas, B. C., and R. W. Agreen, The sea state correction for GEOS 3 and Seasat satellite altimeter data, *J. Geophys. Res.*, **88**, 1655-1661, 1983.
- Dudis, J. J., Electromagnetic bias of airborne off-nadir laser backscatter from the ocean, *J. Geophys. Res.*, **91**, 10,750-10,752, 1986.
- Hayne, G. S., Radar altimeter mean return waveforms from near-normal-incidence ocean surface scattering, *IEEE Trans. Antennas, Propag.*, **AP-28**, 687-692, 1980.
- Hoge, F. E., W. B. Krabill, and R. N. Swift, The reflection of airborne UV laser pulses from the ocean, *Mar. Geod.*, **8**, 313-344, 1984.
- Huang, N. E., and S. R. Long, An experimental study of the surface

- elevation probability distribution and statistics of wind generated waves, *J. Fluid Mech.*, 101, 179–200, 1980.
- Huang, N. E., S. R. Long, C. C. Tung, Y. Yuan, and L. F. Bliven, A unified two-parameter wave spectral model for a general sea state, *J. Fluid Mech.*, 112, 203–224, 1981.
- Huang, N. E., S. R. Long, C. C. Tung, Y. Yuan, and L. F. Bliven, A non-Gaussian statistical model for surface elevation of nonlinear random wave fields, *J. Geophys. Res.*, 88, 7597–7606, 1983.
- Huang, N. E., S. R. Long, L. F. Bliven, and C. C. Tung, The non-Gaussian joint probability density function of slope and elevation for a nonlinear gravity wave field, *J. Geophys. Res.*, 89, 1961–1972, 1984.
- Huang, N. E., S. R. Long, and L. F. Bliven, An experimental study of the statistical properties of wind-generated gravity waves, in *Wave Dynamics and Radio Probing of the Ocean Surface*, edited by O. M. Phillips and Klaus Hasselmann, pp. 129–144, Plenum, New York, 1986.
- Jackson, F. C., The reflection of impulses from a nonlinear random sea, *J. Geophys. Res.*, 84, 4439–4932, 1979.
- Jackson, F. C., W. T. Walton, and P. L. Baker, Aircraft and satellite measurement of ocean wave directional spectra using scanning beam microwave radars, *J. Geophys. Res.*, 90, 987–1004, 1985a.
- Jackson, F. C., W. T. Walton, and C. Y. Peng, A comparison of in situ and airborne radar observations of ocean wave directionality, *J. Geophys. Res.*, 90, 1005–1018, 1985b.
- Kenney, J. E., and E. J. Walsh, A unique radio oceanographic radar, *Memo. Rep. 4086*, 23 pp., Nav. Res. Lab., Washington, D. C., 1978.
- Kenney, J. E., E. A. Uliana, and E. J. Walsh, The surface contour radar, a unique remote sensing instrument, *IEEE Trans. Microwave Theory Tech.*, MTT 27, 1080–1092, 1979.
- Lagerloef, G. S. E., Comment on "On the joint distribution of surface elevations and slopes for a nonlinear random sea, with an application for radar altimetry" by M. A. Srokosz, *J. Geophys. Res.*, 92, 2985–2987, 1987.
- LeVine, D. M., Comparison of  $\sigma^\circ$  obtained from the conventional definition with  $\sigma^\circ$  appearing in the radar equation for a randomly rough surface, *IEEE Trans. Geosci. Remote Sens.*, GE-20, 85–90, 1982.
- Lipa, B. J., and D. E. Barrick, Ocean surface height-slope probability density function from Seasat altimeter echo, *J. Geophys. Res.*, 86, 10,921–10,930, 1981.
- Longuet-Higgins, M. S., The effect of nonlinearities on statistical distributions in the theory of sea waves, *J. Fluid Mech.*, 17, 459–480, 1963.
- Miller, L. S., and G. S. Hayne, Characteristics of ocean-reflected short radar pulses with application to altimetry and surface roughness determination, *Sea Surface Topography From Space*, edited by J. R. Apel, *Tech. Rep. ERL 228-AOML 7*, vol. 1, pp. 12-1–12-32, Natl. Oceanic and Atmos. Admin., Boulder, Colo., 1972.
- Rodriguez, E., Altimetry for non-Gaussian oceans: Height biases and estimation of parameters, *J. Geophys. Res.*, 93, 14,107–14,120, 1988.
- Shapiro, A., E. A. Uliana, and B. S. Yaplee, Radar pulse shape versus ocean wave height, *Sea Surface Topography From Space*, edited by J. R. Apel, *Tech. Rep. ERL 228-AOML 7*, vol. 1, 11-1–11-29, Natl. Oceanic and Atmos. Admin., Boulder, Colo., 1972.
- Srokosz, M. A., On the joint distribution of surface elevation and slopes for a nonlinear random sea, with application to radar altimetry, *J. Geophys. Res.*, 91, 995–1006, 1986.
- Srokosz, M. A., Reply, *J. Geophys. Res.*, 92, 2989–2990, 1987.
- Tayfun, M. A., On narrow-band representation of ocean waves, 1, Theory, *J. Geophys. Res.*, 91, 7743–7752, 1986.
- Walsh, E. J., D. W. Hancock, D. E. Hines, and J. E. Kenney, Electromagnetic bias of 36-GHz radar altimeter measurements of MSL, *Mar. Geod.*, 8, 265–296, 1984.
- Yaplee, B. S., A. Shapiro, D. L. Hammond, B. B. Au, and E. A. Uliana, Nanosecond radar observation of the ocean surface from a stable platform, *IEEE Trans. Geosci. Electron.*, GE-9, 170–174, 1971.

F. C. Jackson, NASA Goddard Space Flight Center, Greenbelt, MD 20771.

R. N. Swift, EG&G Washington Analytical Services Center, Inc., Pocomoke City, MD 21581.

E. A. Uliana, Naval Research Laboratory, Washington, DC 20375.

E. J. Walsh, NOAA Wave Propagation Laboratory, Boulder, CO 80303.

(Received February 6, 1989;  
accepted April 25, 1989.)